Preparation of Flower-like ZnO Nanoparticles in a Cellulose Hydrogel Microreactor

Chengcheng Qin,[a] Shujun Li,[a] Guiquan Jiang,[c] Jun Cao,[b,*] Yuliang Guo,[a] Jiangwei Li,[a] Bin Zhang,[a] and Shiyan Han [a,b,*]

Flower-like zinc oxide (ZnO) nanoparticles were synthesized with sodium hydroxide and zinc acetate in a cellulose hydrogel microreactor (prepared by the inversion method). The samples were characterized by scanning electron microscopy, EDX, x-ray diffractometry, ultraviolet-visible diffuse reflection spectroscopy, and nitrogen adsorption-desorption. The results indicated that ZnO grows in a flower-like shape in the pores of the cellulose hydrogel. The pure hexagonal wurtzite structures have uniform diameters in the range of 10 nm to 30 nm, surface areas of 39.18 m^2/g, and pore volumes of 0.2109 cm^3/g. This study also investigated the photocatalytic properties. The nanoparticles have a band gap of 3.23 eV and a 95.2% efficiency for the ultraviolet degradation of rhodamine B over 3 h at room temperature.

Keywords: Flower-like ZnO; Cellulose hydrogel microreactor; Photocatalytic; Nanoparticle

*Contact information: a: Material Science and Engineering College and b: Postdoctoral Station of Mechanical Engineering, Northeast Forestry University, Harbin 150040, China; c: Forestry College of Beihua University, Jilin 132013, China; *Corresponding author: hanshiyan80@163.com*

INTRODUCTION

Zinc oxide (ZnO) has been widely used in photocatalysts (Han *et al.* 2012), solar cells (Wu *et al.* 2010), transistors (Ong *et al.* 2007), piezoelectric transducers (Choi *et al.* 2010), and gas sensors (Spencer and Yarovsky 2010). The II-VI compound semiconductor has outstanding electrical and optical properties (Cho *et al.* 2009) as well as excellent chemical and thermal stabilities. Zinc oxide has a wide direct band gap at 3.37 eV and an exciton binding energy of 60 meV (Su *et al.* 2010). Due to its high photosensitivity, low cost (Zhu *et al.* 2012), and nontoxicity, ZnO is an important semiconductor photocatalyst. Composite materials with ZnO have better photocatalytic activity under visible light (Shaker-Agjekandy and Habibi-Yangjeh 2016; Shekofteh-Gohari and Habibi-Yangjeh 2016). Generally, the shape, size, and crystalline structure of semiconductors determine their chemical and physical properties. Zinc oxide materials have been prepared with different sizes and morphologies, such as spheres (Deng *et al.* 2008), flower-like shapes (Zhao *et al.* 2007), tubes (Li *et al.* 2008), cages, prismatic shapes, ellipsoidal shapes, hollow shells (Yu and Yu 2008), dumbbell shapes, nanowires (Ghoshal *et al.* 2008), nanorods (Cui *et al.* 2009), and nano-bundles (Muruganandham and Wu 2008). Various methods yield the large variety of shapes, sizes, and crystalline forms, as well as differing optical properties (Colón *et al.* 2008). These methods include hydrothermal synthesis (Hu *et al.* 2008), sol-gel processes (Rani *et al.* 2008), chemical deposition (Lokhande *et al.* 2009), chemical vapor deposition (Hu *et al.* 2012), and gas-phase reactions.

Hydrogels, which are three-dimensional networks of hydrophilic polymers, can

absorb and retain a substantial amount of water. They are formed *via* hydrogen bonds, physical entanglement, chemical cross-linking, and ionic bonds. Due to hydrogels being hydrophilic, permeable, biocompatible, and having a low coefficient of friction, they have been widely used for drug delivery, water-absorbing resins, and cosmetics. Hydrogels prepared from natural polymers, especially polysaccharides, have promising applications as biomaterials because they are abundant, biodegradable, and non-toxic. Cellulose is an abundant, renewable polysaccharide raw material used in hydrogels. Chemical cross-linking, using water-soluble cellulose derivatives and bifunctional cross-linkers, is an elegant route to prepare hydrogels. Synthesizing cellulose-based hydrogels by radiation-induced polymerization is also convenient. Lastly, transparent cellulose hydrogels can be made by cellulose regeneration *via* changing the solution conditions (*i.e.*, pH, temperature). These hydrogels (Isobe *et al.* 2013) are highly porous, with 50 nm to 100 nm pores and large surface areas of 300 m^2/g to 400 m^2/g (Chang *et al.* 2010).

For this study, hydrogels were synthesized with a "one-step" method from unsubstituted cellulose that was dissolved directly in a sodium hydroxide (NaOH)/urea aqueous solution by adjusting the pH and temperature. The cellulose hydrogels were then used as a microreactor for ZnO growth in the pore structure. The ZnO morphology, structure, and performance were characterized.

EXPERIMENTAL

Materials

Bamboo fiber (98% cellulose) was prepared by slicing, steaming, cooking, and enzyme processing. It was purchased from Mingtong Bamboo Charcoal Products Co., Ltd. (Jinhua City, Zhejiang Province, China). Zinc acetate dihydrate ($Zn(CH_3COO)_2 \cdot 2H_2O$), NaOH, urea, anhydrous ethanol, tert-butyl alcohol, and rhodamine B were supplied by Aladdin Industrial Inc. (Shanghai, China). All chemicals were analytical-grade reagents and used without further purification. Deionized water was used throughout the experimentation.

Preparation of Cellulose Hydrogel and ZnO

Regenerated cellulose hydrogel was fabricated by the inversion method. When a 7:12:81 mass ratio solution of NaOH/urea/H_2O (100 g) was cooled to -12 °C, 2.0 g of bamboo fiber was added and dispersed with vigorous stirring for 3 min (Cai *et al.* 2004; Zhou *et al.* 2004). The transparent cellulose solution (5 mL) was then added to a 10-mL sealed beaker and placed in a 50 °C water-bath for 24 h, yielding the cellulose hydrogel (Cai and Zhang 2006).

The hydrogel was transferred to a 100-mL beaker, immersed in 50 mL of water, and washed three times until the pH was 9. The surface water of the hydrogel was exchanged with ethanol *via* flushing. Subsequently, the hydrogel was immersed in a 100 mL of ethanol solution containing 0.1 wt.% zinc acetate for 48 h in a 40 °C water bath. The resulting ZnO precursor/cellulose hydrogel hybrid was washed with ethanol three times, then removing the water in precursor by absolute ethanol 72h and immerging tert-butanol 12 h of 3 times, at last freeze drying. The resulting ZnO precursor/cellulose aerogel hybrid was finally calcined in a muffle furnace in air at 500 °C for 3 h to obtain the flower-like ZnO.

Methods

Scanning electron microscopy (SEM; QUATA200, FEI Company, Hillsboro Oregon, USA) of the cellulose hydrogel, ZnO precursor/cellulose hydrogel hybrid, and ZnO was performed. The purity and elemental analysis of the ZnO were obtained by EDX on the same SEM instrument. X-ray diffractometry (XRD; Rigaku D/max-2200, Tokyo, Japan) was performed with a D/max-rB diffractometer with 40 kV and 30 mA Cu Kα radiation in the 2θ range of 20° to 80°, at a scanning speed of 4°/min. Transmission electron microscopy (TEM) of the ZnO particle size distribution was performed with a H-7650 instrument (Hitachi, Tokyo, Japan). The surface areas were determined from nitrogen adsorption-desorption isotherms using an ASAP 2000 instrument (Coulter Omnisorp 100CX, Beckman Coulter Company, Norcross, GA, USA) and Brunauer-Emmett-Teller (BET) calculations. The UV-visible diffuse reflection spectra of ZnO were acquired on a TU-1901 UV-visible spectrophotometer (equipped with an integrating sphere) (Beijing Purkinje General Instrument Co., Ltd., Beijing, China), using $BaSO_4$ as a reference.

Photocatalytic Activity

The photocatalytic activities of the ZnO nanocrystals were evaluated by monitoring the degradation of rhodamine B in an aqueous solution in a reactor described previously (Sun *et al.* 2009). The ZnO (10 mg) and 200 mL of 10 mg/L rhodamine B solution were placed in the reactor and mixed with an air diffuser, which was placed at the bottom of the reactor to uniformly disperse air into the solution at a flow rate of 0.5 m^3/h. The solution was initially stirred for 30 min to reach absorption equilibrium and was then exposed to 300 W of UV light, with the strongest emission at 365 nm. The reactor was kept at room temperature *via* a water bath. To monitor the rhodamine B degradation, a sample was collected by centrifugation every 30 min and characterized with the UV-visible spectrophotometer set at the 550 nm rhodamine B absorption maximum. For a control experiment, the same reaction without catalyst was monitored under the same conditions.

RESULTS AND DISCUSSION

SEM of Flower-like ZnO and its Formation Mechanism

Figures 1a, b, c, and d show the morphologies of the cellulose hydrogel, the ZnO precursor/cellulose hydrogel hybrid, ZnO, and ZnO at higher magnification, respectively. Notably, the cellulose hydrogel fibers were intertwined with each other forming a porous network structure (Liu *et al.* 2014). The ZnO was grown in the shape of flowers, and this morphology was maintained during roasting in a muffle furnace.

From the SEM images, as well as from previous reports (Zhang and Mu 2007; Kuriakose *et al.* 2013), the formation of flower-like ZnO structures involves three stages, which are shown in Fig. 2. Their growth strongly depends on the concentration of Zn^{2+} and OH^- ions, and it involves the following processes: (1) nucleation and growth of ZnO nanoparticles; (2) oriented attachment of the nanoparticles to form nanosheets; and (3) self-assembly of the nanosheets into three-dimensional flower-like structures. Here, ZnO nanostructures were synthesized from NaOH and zinc acetate in a 40 °C water bath, and the cellulose hydrogel was used as a microreactor. While the cellulose hydrogel was prepared, the NaOH/urea/H_2O solution was used as the solvent system, and the hydrogel

surface water was exchanged with ethanol. Consequently, NaOH, urea, and H_2O were present in the hydrogel pores. After the hydrogel was immersed in the ethanol solution of zinc acetate, the NaOH and zinc acetate reacted as follows (Bian *et al.* 2011; Sun *et al.* 2012).

$$Zn^{2+} + 2OH^- \rightarrow Zn(OH)_2 \quad (1)$$

$$Zn(OH)_2 \rightarrow ZnO + H_2O \quad (2)$$

$$Zn(OH)_2 + 2OH^- \leftrightarrow [Zn(OH)_4]^{2-} \quad (3)$$

$$ZnO + H_2O + 2OH^- \leftrightarrow [Zn(OH)_4]^{2-} \quad (4)$$

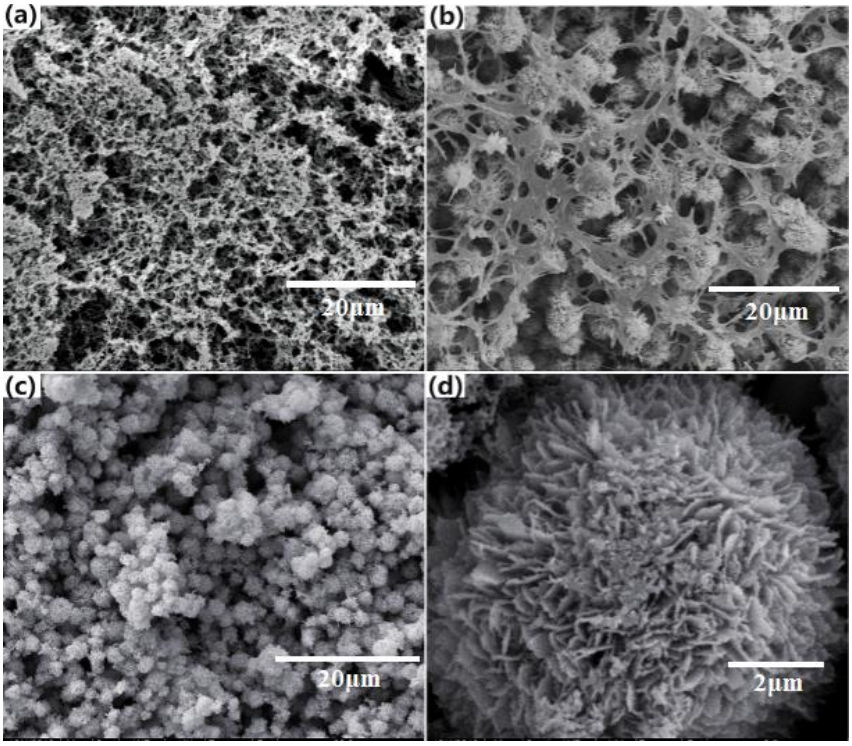

Fig. 1. SEM of the ZnO samples: (a) cellulose hydrogel; (b) ZnO precursor/cellulose hydrogel hybrid; (c) ZnO (×2000); and (d) ZnO (×15000) magnification

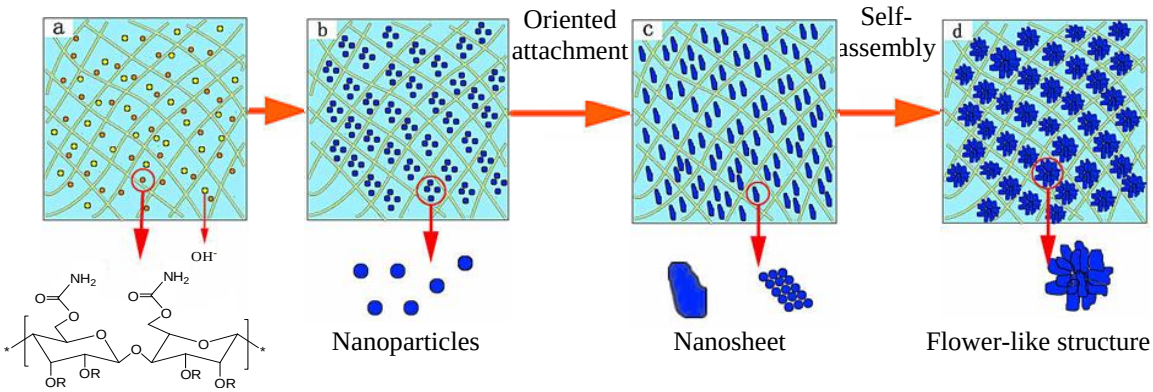

Fig. 2. Formation mechanism of flower-like ZnO structures

Due to the water and the chemical bonding between the NaOH/urea/H_2O and the cellulose hydrogel, the reaction proceeded slowly in the pores. In the presence of excess OH^- ions (a higher NaOH concentration in this case), $[Zn(OH)_4]^{2-}$ ions were formed. The dehydration of $[Zn(OH)_4]^{2-}$ led to the nucleation and growth of ZnO nanoparticles. Subsequently, the urea induced the oriented attachment of the ZnO nanoparticles to form ZnO nanosheets (Wu *et al.* 2005). Finally, to minimize the surface energy the nanosheets were self-assembled into three-dimensional flower-like structures. The uniform pore sizes in the cellulose hydrogel microreactor led to the uniform dimensions of the ZnO structures.

Analysis of XRD and EDX

The XRD patterns of the ZnO sample are shown in Fig. 3a. The high intensities of the diffraction peaks suggest that it was very crystalline (Zhao *et al.* 2013). All peaks matched well with the hexagonal wurtzite structure of ZnO (JCPDS card No. 36-1451). No noticeable impurities were detected; this indicated that the sample was pure ZnO.

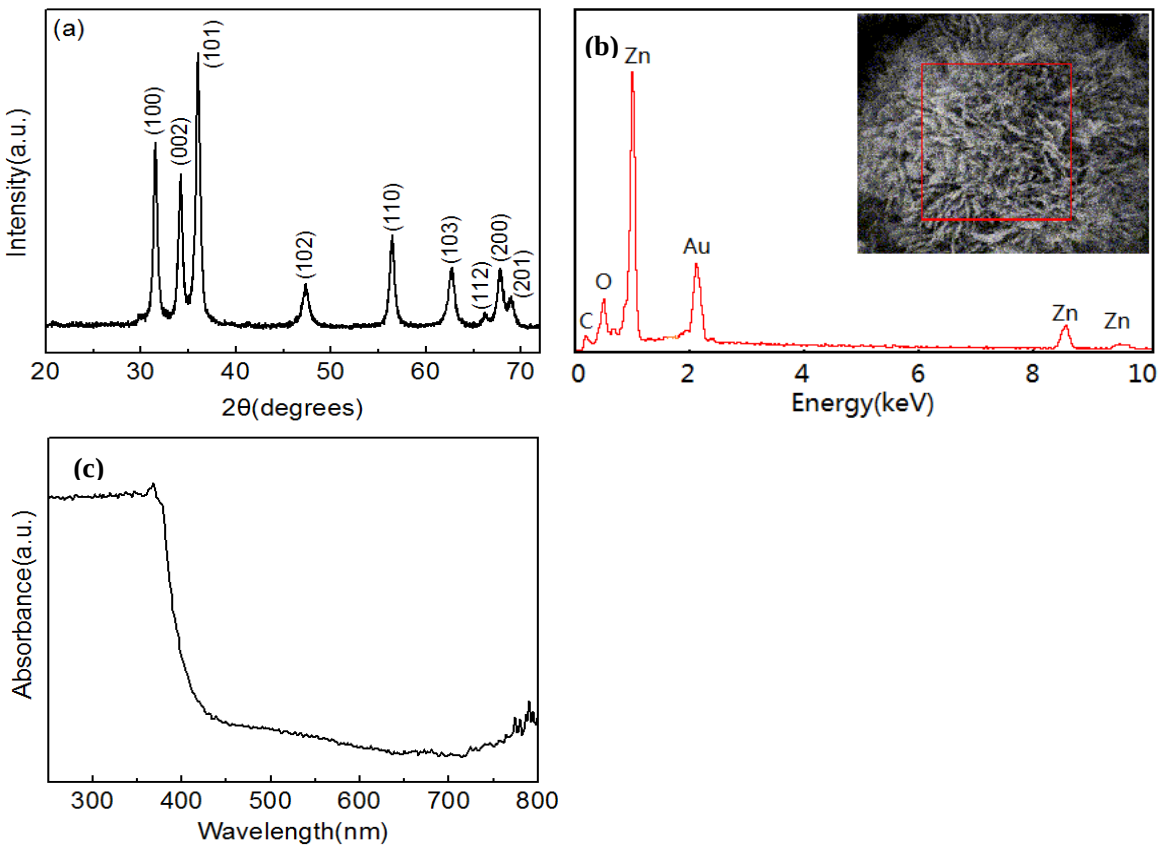

Fig. 3. (a) XRD of the ZnO sample, (b) EDX of the ZnO sample and (c) UV-visible diffuse reflection spectroscopy of the ZnO sample

The purity and elemental analysis of the ZnO were obtained by EDX on the same SEM instrument. As indicated in Fig. 3b, no impurity was detected. The Au element was introduced by SEM (the sample was sprayed with Au) and the C element was mainly due to CO_2 in the air because the prepared ZnO did not show the presence of the C element according to XRD.

UV-Visible Diffuse Reflection Spectroscopy

The absorption of UV and visible light is an important photocatalytic property. As shown in Fig. 3c, the ZnO had a broad absorption band that extended from the ultraviolet to the visible region, with a maximum absorption at 384 nm. This intrinsic band-gap absorption was a result of the electron transitions from the valence to the conduction band. The absence of other bands confirmed the sample purity and indicated a uniform microstructure. The ZnO band gap energy E_{bg} was estimated to be 3.23 eV, according to E_{bg}= 1240/λ (eV) (where λ is the 384-nm absorption maximum), (E_{bg}- Band gap energy of semiconductor eV, λ-Irradiation wavelength threshold nm) (Zhao *et al.* 2013; Venkatachalam *et al.* 2007).

BET Analysis

Figure 4(a) reveals the nitrogen adsorption-desorption isotherms of the ZnO samples. The isotherms were type IV, with H3 hysteresis loops that are characteristic of porous materials. Thus, the samples had a mesoporous texture with a uniform interparticle distribution. The BET analysis indicated a surface area of 39.18 m^2/g, whereas the pore volume, as determined by the Barrett-Joyner-Halenda method, was 0.2109 cm^3/g, with an average pore size of 21.5 nm.

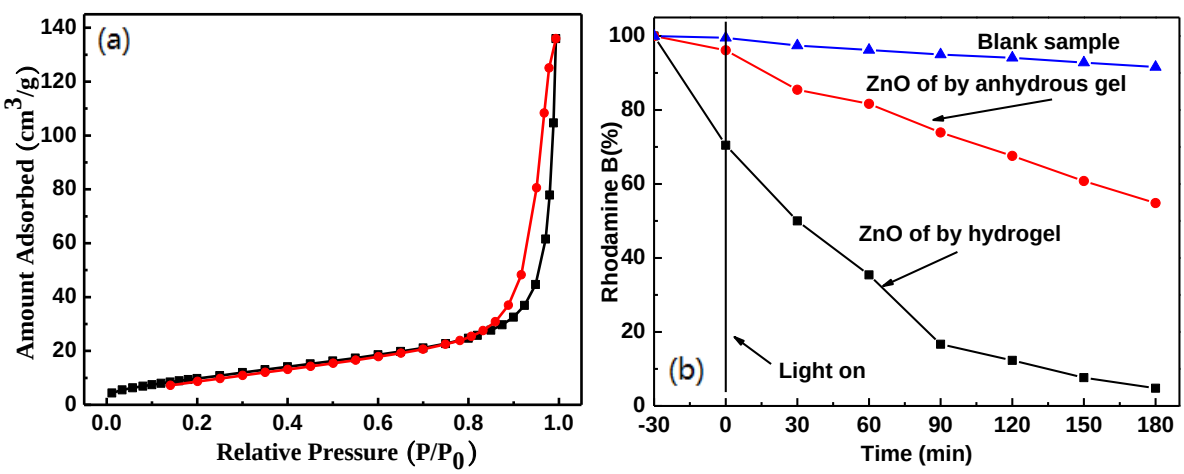

Fig. 4. (a) N_2 adsorption-desorption of the ZnO sample, and (b) photocatalytic degradation curves of RhB over ZnO

Photocatalytic Degradation of Rhodamine B

As shown in Fig. 4b, the concentration of rhodamine B (RhB) did not change over 180 min in the absence of the ZnO photocatalyst, which indicated that the catalyst was essential for efficient photodegradation (Zhao *et al.* 2013). It was also clear that the RhB concentration changed remarkably during the pre-absorption with the UV light off, which may have been due to the large ZnO surface area for the adsorption of RhB (Zhou *et al.* 2012). When the UV light was switched on, the photocatalytic reaction was initiated, and the RhB concentration decreased greatly. After catalyzed 180 min, the degradation rate of rhodamine B by ZnO, with the addition of hydrogel and no hydrogel, was 95.2% and 45.2%, respectively. This good result can be attributed to the preparation of the ZnO sample using the hydrogel as a microreactor. As reported previously, photocatalysts with

higher surface energies exhibit better photocatalytic performances. Moreover, the (0001) plane exhibits the highest surface energy for ZnO (Zhang *et al.* 2007; Xu *et al.* 2009). Thus, the flower-like ZnO nanosheets, which had large areas in the (0001) orientation, exhibited good photocatalytic activities.

CONCLUSIONS

1. With bamboo fiber as raw material, a cellulose hydrogel with uniform pore size was prepared by inverse method, and flower-like ZnO was prepared using the hydrogel as a micro reactor and zinc acetate as raw material.
2. The prepared ZnO using hydrogel as micro reactor exhibited a flower structure with uniform morphology according to SEM. The material was hexagonal wurtzite according to XRD, and it was pure ZnO by EDX. The band gap width was 3.23eV based on UV. The specific surface area and pore volume were 39.18 m^2/g and 0.2109 cm^3/g, respectively.
3. After the process of catalysis had taken place for 180 min, the degradation rate of rhodamine B by ZnO with the addition of hydrogel and without hydrogel was 95.2% and 45.2%, respectively. The results showed that the photocatalytic activity of ZnO using hydrogel as micro reactor was higher.

ACKNOWLEDGMENTS

This work was supported by the Fundamental Research Funds for the Central Universities (2572014CB03), the Young Technology Innovation Talent Foundation of Harbin (2013RFQXJ035), the Young Science Foundation of Heilongjiang (QC2013C033), and the Key Projects of Science and Technology Department of Jilin Province (20140204006GX).

REFERENCES CITED

Bian, S. W., Mudunkotuwa, I. A., Rupasinghe, T., and Grassian, V. H. (2011). "Aggregation and dissolution of 4 nm ZnO nanoparticles in aqueous environments: influence of pH, ionic strength, size, and adsorption of humic acid," *Langmuir* 27(10), 6059-6068. DOI: 10.1021/la200570n

Cai, J., Zhang, L. N., Zhou, J. P., Li, H., Chen, H., and Jin, H. M. (2004). "Novel fibers prepared from cellulose in NaOH/Urea aqueous solution," *Macromol. Rapid Comm.* 25(17), 1558-1562. DOI: 10.1002/marc.200400172

Cai, J., and Zhang, L. N. (2006). "Unique gelation behavior of cellulose in NaOH/Urea aqueous solution," *Biomacromolecules* 7(1), 183-189. DOI: 10.1021/bm0505585

Chang, C. Y., Zhang, L. Z., Zhou, J. P., Zhang, L. N., and Kennedy, J. F. (2010). "Structure and properties of hydrogels prepared from cellulose in NaOH/urea aqueous solutions," *Carbohyd. Polym.* 82(1), 122-127. DOI: 10.1016/j.carbpol.2010.04.033

Cho, S., Jang, J. W., Jung, S. H., Lee, B. R., Oh, E., and Lee, K. H (2009). "Precursor effects of citric acid and citrates on ZnO crystal formation," *Langmuir* 25(6), 3825-3831. DOI: 10.1021/la804009g

Choi, D., Choi, M. Y., Choi, W. M., Shin, H. J., Park, H. K., Seo, J. S., Park, J., Yoon, S. M., Chae, S. J., Lee, Y. H., *et al.* (2010). "Fully rollable transparent nanogenerators based on graphene electrodes," *Adv. Mater*. 22(19), 2187-2192. DOI: 10.1002/adma.200903815

Colón, G., Hidalgo, M. C., Navío, J. A., Melián, E. P., González, D. O., and Dona Rodríguez, J. M. (2008). "Highly photoactive ZnO by amine capping-assisted hydrothermal treatment," *Appl. Catal. B-Environ*. 83(1-2), 30-38. DOI: 10.1016/j.apcatb.2008.01.033

Cui, Q. Y., Huang, Y., and Zhu, Z. Q. (2009). "Synthesis and field emission of novel ZnO nanorod chains," *Current Applied Physics* 9(2), 426-430. DOI: 10.1016/j.cap.2008.03.011

Deng, Z. W., Chen, M., Gu, G. X., and Wu, L. M. (2008). "A facile method to fabricate ZnO hollow spheres and their photocatalytic property," *J. Phys. Chem. B* 112(1), 16-22. DOI: 10.1021/jp077662w

Ghoshal, T., Biswas, S., Kar, S., Dev, A., Chakrabarti, S., and Chaudhuri, S. (2008). "Direct synthesis of ZnO nanowire arrays on Zn foil by a simple thermal evaporation process," *Nanotechnology* 19(6), 2222-2229. DOI: 10.1088/0957-4484/19/6/065606

Han, Z. Z., Liao, L., Wu, Y. T., Pan, H. B., Shen, S. F., and Chen, J. Z. (2012). "Synthesis and photocatalytic application of oriented hierarchical ZnO flower-rod architectures," *J. Hazard. Mater*. 217-218(6), 100-106. DOI: 10.1016/j.jhazmat.2012.02.074

Hu, X. L., Masuda, Y., Ohji, T., and Kato, K. (2008). "Semi-circular shaped ZnO nanowhiskers assemblies deposited using an aqueous solution," *Appl. Surf. Sci*. 255(5), 2329-2332. DOI: 10.1016/j.apsusc.2008.07.093

Hu, P., Han, N., Zhang, D. W., Ho, J. C., and Chen, Y. F. (2012). "Highly formaldehyde-sensitive, transition-metal doped ZnO nanorods prepared by plasma-enhanced chemical vapor deposition," *Sensor. Actuat. B-Chem*. 169(4), 74-80. DOI: 10.1016/j.snb.2012.03.035

Isobe, N., Chen, X. X., Kim, U. J., Kimura, S., Wada, M., Saito, T., and Isogai, A. (2013). "TEMPO-oxidized cellulose hydrogel as a high-capacity and reusable heavy metal ion adsorbent," *J. Hazard. Mater*. 260C(1), 195-201. DOI: 10.1016/j.jhazmat.2013.05.024

Kuriakose, S., Bhardwaj, N., Singh, J., Satpati, B., and Mohapatra, S. (2013). "Structural, optical, and photocatalytic properties of flower-like ZnO nanostructures prepared by a facile wet chemical method," *Beilstein Journal of Nanotechnology* 4, 763-770. DOI: 10.3762/bjnano.4.87

Li, C. Q., Li, Y., Luo, L. T., and Fu, M. G. (2008). "Synthesis and characterization of ZnO microcrystal tubes," *Journal of the Chilean Chemical Society* 53(3), 1615-1616. DOI: 10.4067/S0717-97072008000300014

Liu, Z. M., Yang, S. L., and Wu, P. (2014). "Characterization of spherical mesoporous aerogels from regenerated bamboo fiber," *Science and Technology Review* 32(4/5), 69-73. DOI:10.3981/j.issn.1000-7857.2014.h1.011

Lokhande, C. D., Gondkar, P. M., Rajaram, S. M., Shinde, V. R., and Han, S. H. (2009). "CBD grown ZnO-based gas sensors and dye-sensitized solar cells," *J. Alloy. Compd.* 475(1-2), 304-311. DOI: 10.1016/j.jallcom.2008.07.025

Muruganandham, M., and Wu, J. J. (2008). "Synthesis, characterization and catalytic activity of easily recyclable zinc oxide nanobundles," *Appl. Catal. B-Environ.* 80(1-2), 32-41. DOI: 10.1016/j.apcatb.2007.11.006

Ong, B. S., Li, C. S., Li, Y. N., Wu, Y. L., and Loutfy, R. (2007). "Solution-processed, high-mobility ZnO thin-film transistors," *J. Am. Chem. Soc*. 129(10), 2750-2751. DOI: 10.1021/ja068876e

Rani, S., Suri, P., Shishodia, P. K., and Mehra, R. M. (2008). "Synthesis of nanocrystalline ZnO powder *via* sol-gel route for dye-sensitized solar cells," *Sol. Energ. Mat. Sol. C*. 92(12), 1639-1645. DOI: 10.1016/j.solmat.2008.07.015

Shaker-Agjekandy, S., and Habibi-Yangjeh, A. (2016). "Ultrasonic-assisted preparation of novel ternary ZnO/AgI/Ag_2CrO_4 nanocomposites as visible-light-driven photocatalysts with excellent activity," *Materials Science in Semiconductor Processing* 44, 48-56. DOI: 10.1016/j.mssp.2015.12.025

Shekofteh-Gohari, M., and Habibi-Yangjeh, A. (2016)." Photosensitization of Fe_3O_4/ZnO by AgBr and Ag_3PO_4 to fabricate novel magnetically recoverable nanocomposites with significantly enhanced photocatalytic activity under visible-light irradiation," *Ceramics International* 42(14), 15224-15234. DOI: 10.1016/j.ceramint.2016.06.158

Spencer, M. J. S., and Yarovsky, I. (2010). "ZnO nanostructures for gas sensing: Interaction of NO_2, NO, O, and N with the ZnO(1010) surface," *J. Phys. Chem. C* 114(24), 10881-10893. DOI: 10.1021/jp1016938

Su, Y. K., Peng, S. M., Ji, L. W., Wu, C. Z., Cheng, W. B., and Liu, C. H. (2010). "Ultraviolet ZnO nanorod photosensors," *Langmuir* 26(1), 603-606. DOI: 10.1021/la902171j

Sun, J. H., Dong, S. Y., Wang, Y. K., and Sun, S. P. (2009). "Preparation and photocatalytic property of a novel dumbbell-shaped ZnO microcrystal photocatalyst," *J. Hazard. Mater*. 172(2-3), 1520-1526. DOI: 10.1016/j.jhazmat.2009.08.022

Sun, Y. J., Wang, L., Yu, X. Q., and Chen, K. Z. (2012). "Facile synthesis of flower-like 3D ZnO superstructures *via* solution route," *CrystEngComm* 14(9), 3199-3204. DOI: 10.1039/C2CE06335B

Venkatachalam, N., Palanichamy, M., and Murugesan, V. (2007). "Sol–gel preparation and characterization of alkaline earth metal doped nano TiO_2: Efficient photocatalytic degradation of 4-chlorophenol," *Journal of Molecular Catalysis A: Chemical* 273(1-2), 177-185. DOI: 10.1016/j.molcata.2007.03.077

Wu, J. J., Chen, Y. R., Liao, W. P., Wu, C. T., and Chen, C. Y. (2010). "Construction of nanocrystalline film on nanowire array *via* swelling electrospun polyvinylpyrrolidone-hosted nanofibers for use in dye-sensitized solar cells," *ACS Nano*. 4(10), 5679-5684. DOI: 10.1021/nn101282w

Wu, G. S., Xie, T., Yuan, X. Y., Li, Y. Z., Yang, L. J., Xiao, Y. H., and Zhang, L. D. (2005). "Controlled synthesis of ZnO nanowires or nanotubes *via* sol-gel template process," *Solid State Commun.* 134(7), 485-489. DOI: 10.1016/j.ssc.2005.02.015

Xu, L. P., Hu, Y. L., Pelligra, C., Chen, C. H., Jin, L., Huang, H., Sithambaram, S., Aindow, M., Joesten, R., and Suib, S. L. (2009). "ZnO with different morphologies synthesized by solvothermal methods for enhanced photocatalytic activity," *Chem. Mater*. 21(13), 2875-2885. DOI: 10.1021/cm900608d

Yu, J. G., and Yu, X. X. (2008). "Hydrothermal synthesis and photocatalytic activity of zinc oxide hollow spheres," *Environ. Sci. Technol*. 42(13), 4902-4907. DOI: 10.1021/es800036n

Zhang, Y. Y., and Mu, J. (2007). "Controllable synthesis of flower-and rod-like ZnO nanostructures by simply tuning the ratio of sodium hydroxide to zinc acetate," *Nanotechnology* 18(7), 3205-3210. DOI: 10.1088/0957-4484/18/7/075606

Zhang, J., Sasaki, K., Sutter, E., and Adzic, R. R., (2007). "Stabilization of platinum

oxygen-reduction electrocatalysts using gold clusters," *Science* 315(5809), 220-222. DOI: 10.1126/science.1134569

Zhao, X. H., Li, M., and Lou, X. D. (2013). "Sol-gel assisted hydrothermal synthesis of ZnO microstructures: Morphology control and photocatalytic activity," *Adv. Powder Technol.* 25(1), 372-378. DOI: 10.1016/j.apt.2013.06.004

Zhao, J. W., Qin, L. R., Xiao, Z. D., and Zhang, L. D. (2007). "Synthesis and characterization of novel flower-shaped ZnO nanostructures," *Mater. Chem. Phys*. 105(2), 194-198. DOI: 10.1016/j.matchemphys.2007.04.031

Zhou, X., Shi, T. J., and Zhou, H. O. (2012). "Hydrothermal preparation of ZnO-reduced graphene oxide hybrid with high performance in photocatalytic degradation," *Appl. Surf. Sci.* 258(17), 6204-6211. DOI: 10.1016/j.apsusc.2012.02.131

Zhou, J. P., Zhang, L. N., and Cai, J. (2004). "Behavior of cellulose in NaOH/Urea aqueous solution characterized by light scattering and viscometry," *J. Polym. Sci. Pol. Phys.* 42(2), 347-353. DOI: 10.1002/polb.10636

Zhu, C. Q., Lu, B. G., Su, Q., Xie, E. Q., and Lan, W. (2012). "A simple method for the preparation of hollow ZnO nanospheres for use as a high performance photocatalyst," *Nanoscale* 4(10), 3060-3064. DOI: 10.1039/C2NR12010K

Article submitted: October 23, 2016; Peer review completed: December 13, 2016; Revised version received: March 4, 2017; Accepted: March 5, 2017; Published: March 13, 2017.
DOI: 10.15376/biores.12.2.3182-3191